

## Analyzing the Performance of EBF Links Using Linear and Quadratic Solid Elements

Musbar<sup>1</sup>, Jufriadi<sup>2,\*</sup>, Khairul Miswar<sup>1</sup>, Munardy<sup>1</sup>, Hanif<sup>1</sup>

<sup>1</sup>Civil Engineering Department, Politeknik Negeri Lhokseumawe, Indonesia

<sup>2</sup>Mechanical Engineering Department, Politeknik Negeri Lhokseumawe, Indonesia

\*Corresponding author: jufriadi@pnl.ac.id

Received : 10 July 2023

Accepted : 30 July 2023

Online : 5 August 2023

---

**Abstract** – The Eccentrically Braced Frame (EBF) system is widely employed for dissipating seismic energy in high seismic areas due to its ease of design, construction, and exceptional performance. EBF structures show excellent performance in dissipating the earthquake energy for excellent ductility and strength parameters compared to MRF and CBF structural types. Analytical studies of experimental EBF structures require enormous resources in terms of funding, equipment, time, and a high risk of failure. Numerical analysis is an alternative step for research on EBF structures that can be carried out on a full scale, in contrast to experimental research that can only be carried out on a model or sub-assembled scale. The choice of element type in numerical applications is a very important study. Consideration of data accuracy and cheap resources are the main considerations. In this research, a study was conducted on the earthquake energy dissipation element, namely the link in the EBF structure, by observing the difference in the use of solid (3D) element types, namely linear and quadratic elements, using the ANSYS 2023 R1 software application. The element size in the link specimen uses a uniform size, with differences in the size and type of elements in each link specimen. The number of link specimens analyzed was 8 pieces, with each element type consisting of 4 pieces. The results showed that link specimens with quadratic elements and small element sizes showed excellent results compared to link specimens with linear elements of the same element size. The accuracy of the results obtained from the quadratic element specimens is mainly in the reading of strain and stress values in the critical zone. For the structural performance on the variables of strength, overstrength and plastic rotation angle obtained in all the analyzed link specimens showed relatively similar results. The results show that the use of linear elements with small element sizes gives excellent results and is more efficient than the use of quadratic elements.

**Keywords:** linear element, quadratic element, overstrength, plastic rotation

---

### Introduction

EBF is one of the most widely used structural systems for the dissipation of seismic energy. It is a very attractive option for structural engineers to use in high seismic areas because of its ease of design and construction and its excellent performance. In EBF structures, the failure of the structure during strong earthquake forces is directed to the small elements, called links, and the other elements do not fail. Currently, the research on linking elements in EBF structures continues to progress significantly. Research on EBFs began in the 1980s. It was based on the work of several researchers. Based on the link performance, Popov in the description of his research describes the type of link element based on the location of plastification that (Lian et al., 2020; Tian et al., 2018) occurs. Research on link elements in EBF structures is carried out in two models, namely, experimental and simulation with finite element analysis. Experimental research is conducted on a full model scale or on a submodel scale. Research in the form of a simulation model with the use of the principles of detailed finite element analysis is carried out in order to study the correlation of the results of the research carried out experimentally. In this paper, an overview of this program is presented with an emphasis on analytical studies. Experimental research has shortcomings, including high cost, long time, and limited number of test specimens. To overcome these shortcomings, research using simulation models is a solution to overcome the

shortcomings of the experimental research model. For a large number of specimens, numerical simulation can describe the behavior of the EBF structure. The research of the numerical simulation model is much cheaper and takes less time in comparison with the experimental research models. Numerical simulation research is based on the principle of finite element analysis using computer software. The model used in this study is a numerical simulation model that uses the ANSYS Workbench 2023 R1 software. The numerical analysis results are in good agreement with the experimental test results, including the hysteretic behaviors and failure modes, indicating that the finite element method is a reliable way to analyze the seismic performance and failure modes of structures subjected to earthquakes (Lian et al., 2020; Tian et al., 2018). Some recent studies on link elements and EBF structures with numerical analysis observations show excellent results, namely (Della Corte & Cantisani, 2022; Egan et al., 2017; Ghadami et al., 2021; Mohammad Moradi et al., 2020; Mohebkhah & Azandariani, 2020; Ramonell & Chacón, 2021; Zimbru et al., 2017).

## Materials and Methods

### 1. Material Properties

The steel profile used in this study for the link element is WF 200x100x5.5x8. The steel used is a product manufactured in Indonesia, which is widely available in the market. Tensile steel tests conducted yielded results for yield stress, ultimate stress, yield strain, ultimate strain, and elongation variables shown in Table 1. A comparison of the stress-strain curves of the WF profile obtained by monotonic tensile testing and mathematical modeling for input to the ANSYS application using the cyclic approach model of Kauffman, et al (2001) is shown in Figure 1. Data from the results of tensile tests on steel and mathematical modeling of the stress-strain relationship as input to the ANSYS application using data from the research conducted by Musbar.

Table 1. Stress, strain, and elongation of steel

Section	$F_y$ (MPa)	$F_u$ (MPa)	$\epsilon_y$ (mm/mm)	$\epsilon_u$ (mm/mm)	Elong. (%)
Web	487.64	595.61	0.0027	0.1166	16.05
Flange	401.45	540.08	0.0019	0.1721	24.55

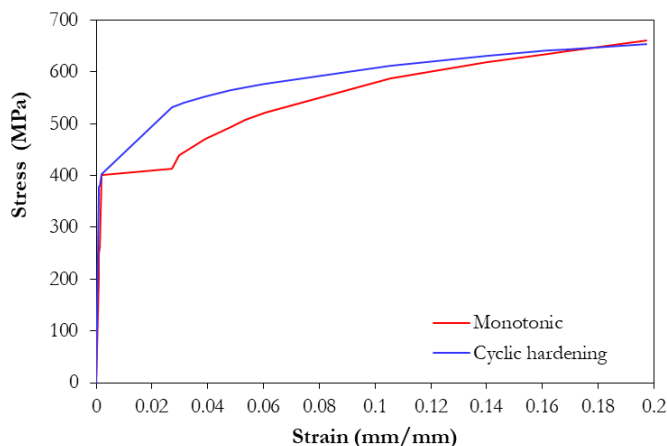


Figure 1. Nominal properties of I-shaped sections

### 2. Boundary Conditions and Loading Pattern

The real condition of the link elements in the EBF structure will be reflected by selecting appropriate boundary conditions and loading. In the initial stage of the research, the numerical simulation of the EBF link element is performed using the concept of boundary conditions proposed by (Richards & Uang, 2005). In this

concept, a force is applied to the right end of the link by the release of displacement in the transverse direction. The left end of the link where the nodes can translate in the longitudinal direction but are forced together to translate in the longitudinal direction. Such a loading model will result in a constant shear force along the link with equal end moments and no axial force generated. Several subsequent studies analyzed the use of boundary conditions with full restraint at one end and a release of one degree of freedom in the longitudinal direction at the other end. The influence of axial forces is eliminated by this boundary condition (Della Corte et al., 2013; Dusicka & Lewis, 2010; Musbar et al., 2018; Stephens & Dusicka, 2014a, 2014b).

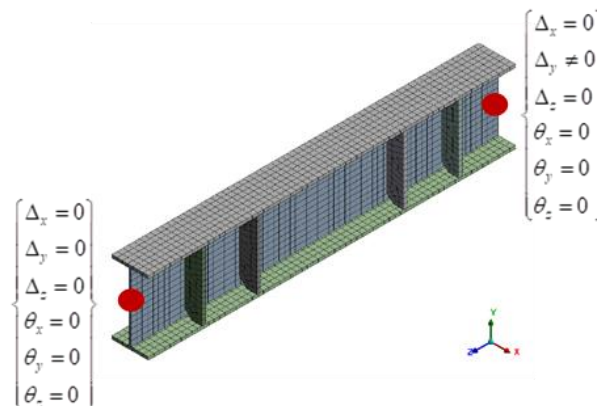


Figure 2. Boundary Conditions

The loading pattern applied to the specimens during testing was adapted to the loading sequence specified in AISC 341-16 Seismic Provisions for Structural Steel Buildings. The force applied to the specimens is determined by the total angle of rotation of the links. Using the requirements of AISC 341-16, as shown in Figure 3.a, the applied load is based on the displacement control that is applied to the link specimens for each load step, as shown in Figure 3.b.

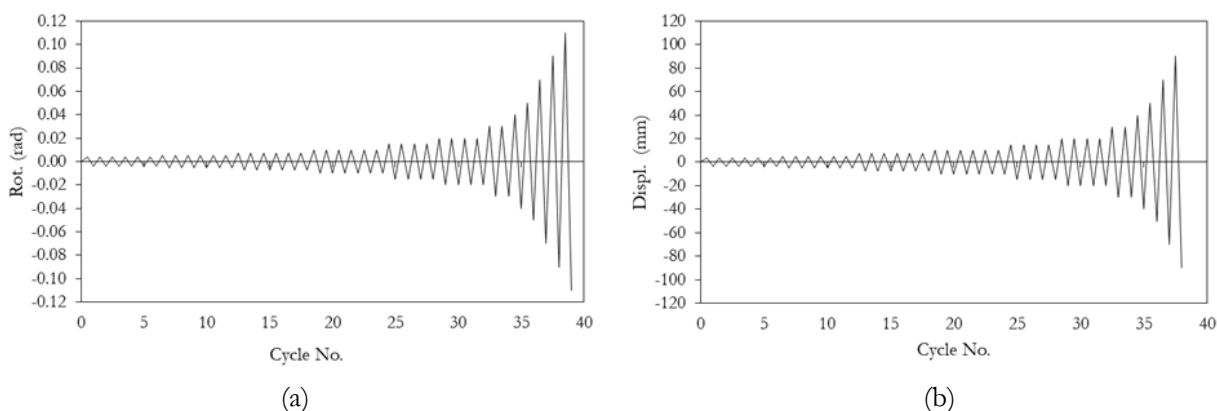


Figure 3. Loading pattern according to aisc 341-16, (a) based on rotation angle, (b) based on displacement

### 3. Specifications of link model

The nonlinear finite element method was used numerically for this study. The test specimen of the link was modeled as a solid element by using the computer software ANSYS 2023 R1. The behavior of the link model was predicted globally, and the strength degradation was obtained at the buckling of the flange, the web, and the web stiffeners of the link specimen control of critical strain values. The strength degradation is related to the fracture or tearing state of the material beyond the limits considered in this study. Geometry nonlinearity

accounts for the large deformations and strains that occur in the analysis of the modeled link specimens. Local instabilities in the link specimen due to the influence of low cycle fatigue, weld cracking, and others were not considered. The yield criterion uses the von Mises criterion with a hardening rule that is multilinear kinematic. The material property data used in the numerical analysis are steel material data from tensile tests. The element selection in ANSYS software for solid elements is divided into two types, namely Linear and Quadratic. The link specimens examined in this study fall into the long link category. Link specimen properties using WF 200x100x5.5x8 steel section and the link length ratio used is 2.96, as shown in Table 2. Based on AISC 341 requirements for links with a link length ratio ( $\rho$ ) greater than 2.5, it is included in the long link category. The width of the web stiffener should not be less than  $(b_f - 2t_w)$  and the thickness should not be less than  $0.75t_w$  or 10 mm, and the maximum web stiffener spacing is  $1.5 b_f$ . In this study, a web stiffener with a thickness of 10 mm and a spacing of 150 mm is used. To prevent and delay the occurrence of fracture in the web, the K-area zone is stopped at a distance of  $4-5t_w$ , which is assumed to be 20 mm.

Table 2. Properties of Link Specimen

Nominal Size	d (mm)	$b_f$ (mm)	$t_w$ (mm)	$t_f$ (mm)	$Z_p$ (mm <sup>3</sup> )	$M_p = Z_p \cdot F_y$ (kN.m)	$V_p = 0,6 \cdot h_w \cdot t_w \cdot F_y$ (kN)	$M_p/V_p$ (mm)	$e = \rho \cdot M_p/V_p$ (mm)	$\rho$	$2 \cdot M_p/e$ (kN)	$V_n = \text{Min}(V_p, 2M_p/e)$ (kN)
200x100	200	100	5.5	8	205000.00	82.30	243.76	337.62	1000	2.96	164.60	164.60

## Data collection

The specimen links analyzed in this study are divided into two solid element types, linear and quadratic. Each type of element consists of four sample links with different element sizes, 7.50 mm, 10.00 mm, 12.50 mm, and 15.00 mm. The element size is set so that the size is uniform across all sample links. This study did not analyze the placement of non-uniform element sizes, especially in the critical and non-critical strain zones. The observation of the specimen links is based on global behavior only. The element size, number of nodes, and elements in the analyzed specimen links are shown in Table 3. The number of elements in the sample links between linear and quadratic element types with the same element size shows similar values, but there is a sharp difference in the number of nodes. The number of nodes in the specimen link with the quadratic element type is more than three times higher than the number of nodes in the specimen link with the linear element type. The selection of parameters that affect the nonlinear behavior of the material used in this study uses the concept of material plasticity as provided by ANSYS. There are several options available. The material plasticity model selection option is appropriate because the material used in this study is a steel material that behaves as a plastic material. Since the plastic behavior of the material is non-conservative and path independent, the response to the applied force is very important for the response of the material used. To obtain an accurate plastic behavior response by considering the time duration of software execution on the computer, this study uses a small incremental force increase in the range of 25-50 steps for the entire load steps. The kinematic hardening model was used to describe the Bauschinger effect on the steel material used in this study. There are two options for kinematic hardening models, namely bilinear kinematic hardening, and multilinear kinematic hardening, in this study the multilinear kinematic hardening model is used.

Table 3. Link Specimens Based on Element Order

No	Specimen	Element Order	Element Size (mm)	Statistics	
				Nodes	Elements
1	QUA01	Quadratic	7.50	85058	13606
2	QUA02	Quadratic	10.00	35548	4700
3	QUA03	Quadratic	12.50	23356	3024
4	QUA04	Quadratic	15.00	16940	2161
5	LIN01	Linear	7.50	24066	13606
6	LIN02	Linear	10.00	10468	4700
7	LIN03	Linear	12.50	6932	3024
8	LIN04	Linear	15.00	5056	2161

## Results

### 1. Performance of Test Specimens

Equivalent plastic stress and strain values obtained in the link specimens for the quadratic and linear element types show relatively small differences. However, because of the different element sizes used in both element types, the specimens show significant differences in strain and stress values. The larger the element size used, the greater the range of differences in values, especially after the link specimen passes the yield condition at 0.01 rad of rotation. The equivalent plastic strain and stress values of the test specimens are shown in Figures 4-7. Specimens QUA01 and LIN01 with 7.5 mm element size can clearly illustrate when the specimens fail. The failure of the specimens was caused by buckling and fracture that occurred in the web at the ends of the link specimens, as shown in Figure 8. Based on the analysis results, the initiation of failure in all specimens showed the same location on the wing at the ends of the link. The buckling behavior in all specimens began to appear after loading at an angle of rotation of 0.02 rad. As the load increases, the buckling that occurs increases until the specimens fail. In general, all specimens did not reach the 0.07 rad angle of rotation when they failed; the angle of rotation reached was 0.05 rad. Specimens QUA01 and LIN01 showed better sensitivity in predicting the failure behavior compared to the other specimens. Comparison of the behavior of specimens QUA01 and LIN01 using von Mises equivalent plastic strain values as shown in Figure 8. Based on the hysteretic curves of shear force versus plastic rotation angle of the specimen link as shown in Figures 9-10, there is a relatively small difference based on the element size for each element type. The hysteretic curves of both element types of specimens using the stress-strain curves of steel tensile test results based on Kaufmann's cyclic model approach show thick, stable, and excellent illustration of the Bauschinger effect.

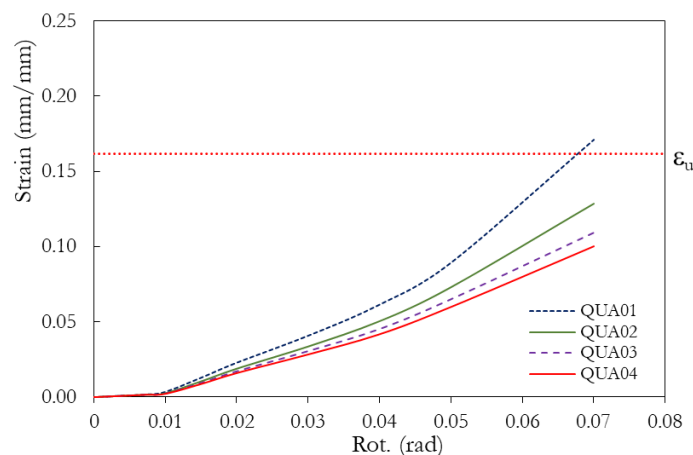


Figure 4. Comparing the Plastic Strain of Link Specimens with Quadratic Element

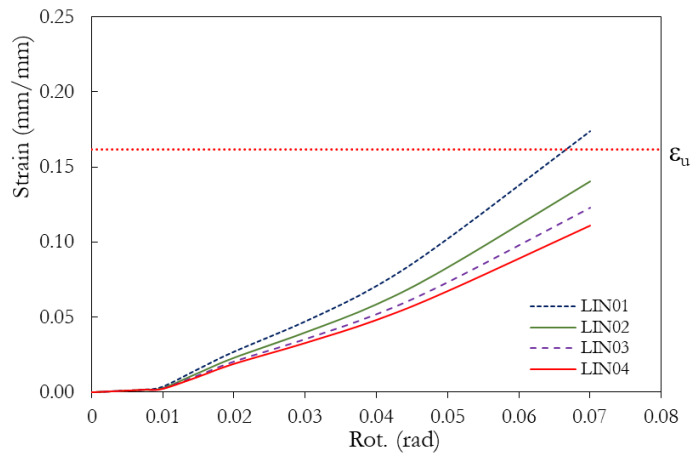


Figure 5. Comparing the Plastic Strain of Link Specimens with Linear Element

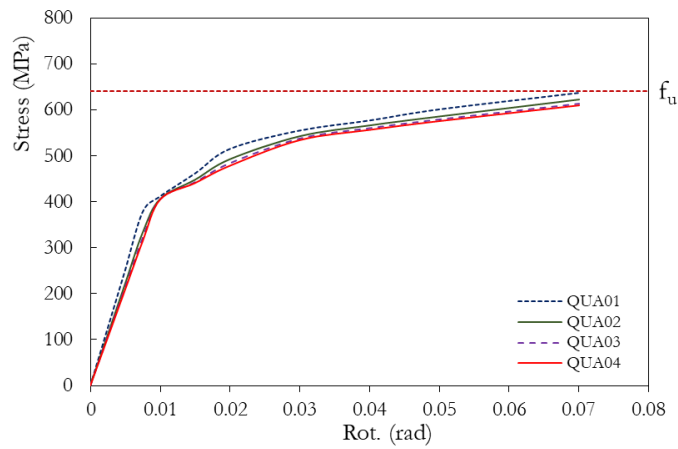


Figure 6. Comparing the Plastic Stress of Link Specimens with Quadratic Element

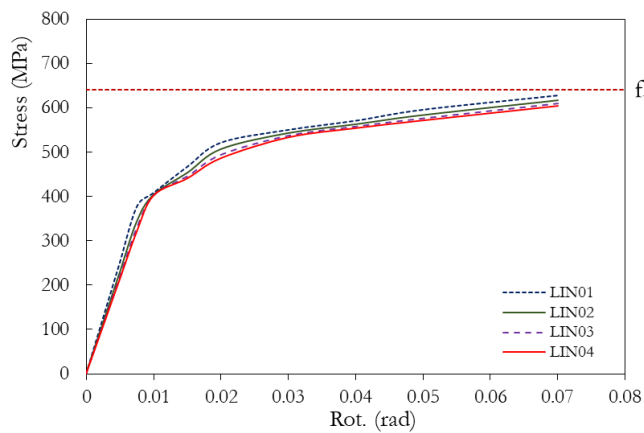


Figure 7. Comparing the Plastic Stress of Link Specimens with Linear Element

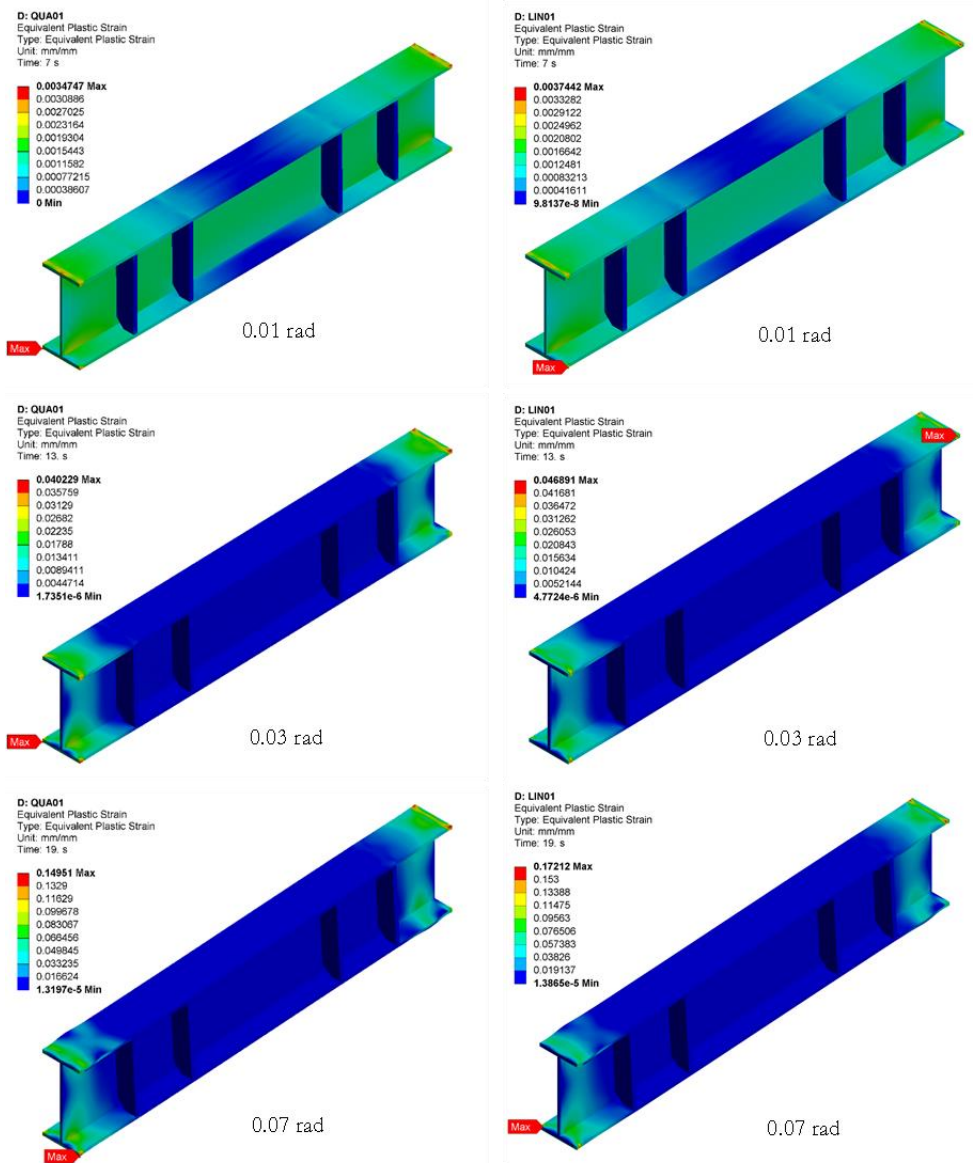


Figure 8. Comparing von Mises Equivalent Plastic Strain of QUA01 and LIN01 Link Specimens

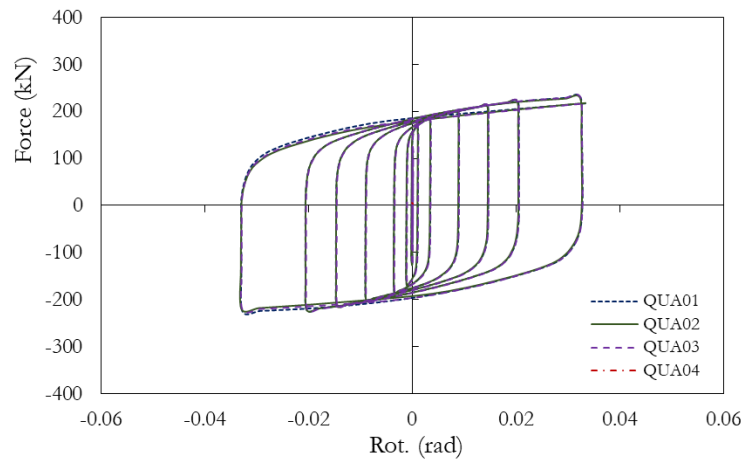


Figure 9. Comparing the Hysteretic Curves of Link Specimens with Quadratic Element

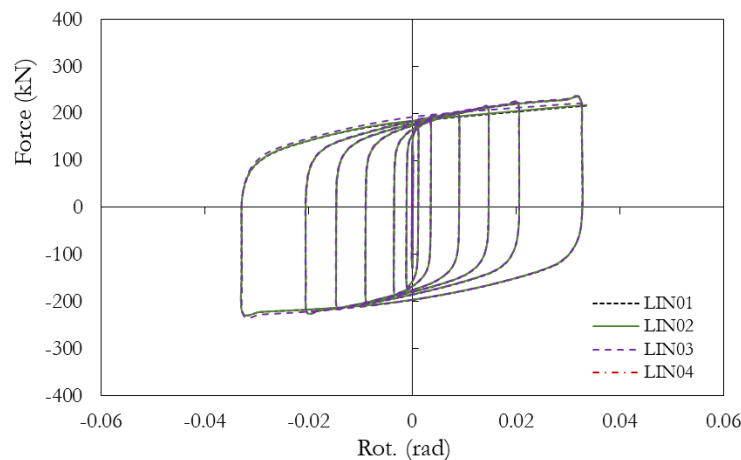


Figure 10. Comparing the Hysteretic Curves of Link Specimens with Linear Element

## 2. Overstrength and Plastic Rotation

The value of the overstrength factor in the link specimens is the ratio of the ultimate shear force ( $V_u$ ) to the plastic shear strength ( $V_p$ ). The value of plastic shear strength of the link specimens is based on the cross-sectional properties of the link using the steel section WF 200x100x5.5x8 as shown in Table 2. The distribution of data on the value of the overstrength factor for link specimens with different types and sizes of elements is shown in Table 4. Based on the value of the overstrength factor, it shows almost the same value with a relatively small difference between specimens. The value of the overstrength factor for link specimens with quadratic element types shows almost the same value in the range of 1.39 - 1.40, while for link specimens with linear element types with a value range of 1.41 - 1.42. The requirements of AISC 341 limit the value of the overstrength factor for the design of elements outside the link to 1.25 for all types of links. In general, the value of the overstrength factor is slightly lower for link specimens with quadratic element types than for link specimens with linear element types. This is due to the different ultimate shear force values obtained from the two types of link elements. The ultimate shear force values of quadratic element link specimens are lower than those of linear element link specimens. In general, the ultimate shear force values of the link specimens for both types of elements show relatively different values depending on the size of the element used. The smaller the element used, the more reduced the shear force value generated. The plastic rotation angle values generated for all the specimens with linear and quadratic element types show values that are almost close to the 0.033 - 0.034 rad

value interval. The achieved plastic rotation value exceeds the requirement of AISC 341 for the long link category, which is 0.02 rad. The obtained plastic rotation angles of link specimens with linear and quadratic element types are shown in Table 4.

Table 4. Overstrength and Plastic Rotation

No.	Specimen	$V_{max}$ (kN)	$V_n$ (kN)	Overstrength ( $V_{max}/V_n$ )	Rot. (rad)	
					Required	Test
1	QUA01	230.66	164.60	1.40	0.020	0.034
2	QUA02	228.89	164.60	1.39	0.020	0.033
3	QUA03	230.41	164.60	1.40	0.020	0.034
4	QUA04	230.73	164.60	1.40	0.020	0.033
5	LIN01	231.51	164.60	1.41	0.020	0.034
6	LIN02	231.29	164.60	1.41	0.020	0.034
7	LIN03	231.89	164.60	1.41	0.020	0.033
8	LIN04	233.01	164.60	1.42	0.020	0.033

Based on the results of the analysis, it can be seen that the smaller the element used, the more accurate the results, but the longer the analysis time. Using linear elements with smaller sizes is more advantageous than using quadratic elements that are smaller or slightly larger. To analyze more specimens and obtain global results, analysis using linear elements is more advantageous than using quadratic elements. The use of linear elements of different sizes, such as finer elements in the zone of possible critical strains that cause failure in the specimen link and coarser elements in the non-critical zone, will have a very good influence on the analysis results. A comparison of the use of various sized elements between quadratic elements and smoothed linear elements is illustrated in Figure 11.

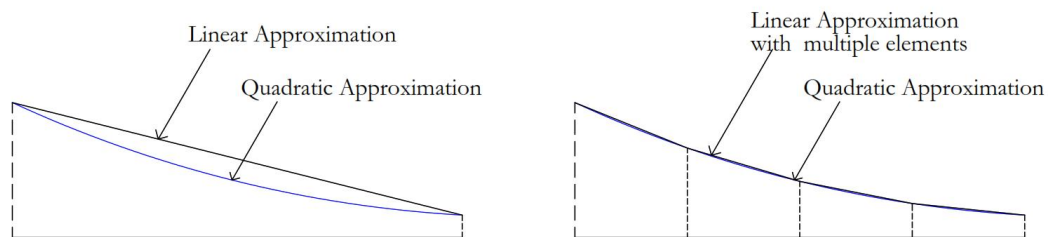


Figure 11. Element order comparison

## Conclusion

Based on the results obtained from the analysis of link specimens using linear and quadratic elements, it can be concluded as follows.

1. Both link elements with element types, namely linear and quadratic, can describe well the yield condition, initial buckling, and failure of the link.
2. The ultimate shear force, overstrength and plastic rotation of all link specimens show almost the same values.
3. The link specimens with the smallest element size showed better accuracy in reading the values of equivalent plastic strain and stress compared to the link specimens with larger element size.
4. For the needs of analyzing more specimen links and the need for faster time and getting a global overview of the analysis results, the analysis using linear elements is more advantageous than using quadratic elements.
5. The use of quadratic elements gives slightly better results than the use of linear elements, but the analysis takes more time.

6. The use of linear elements of various sizes in the test specimens is advantageous. In critical zones, linear elements can be applied more finely than non-critical areas, which can give accurate results as using quadratic elements.

### Acknowledgment

Thanks to Civil Engineering Department and Mechanical Engineering Department, Politeknik Negeri Lhokseumawe, Indonesia for providing support in the implementation of this research activity.

### References

- Della Corte, G., & Cantisani, G. (2022). FEM Analysis of Steel Eccentric Braces for Seismic Retrofitting. *Procedia Structural Integrity*, 44, 472–479. <https://doi.org/10.1016/j.prostr.2023.01.062>
- Della Corte, G., D’Aniello, M., & Landolfo, R. (2013). Analytical and numerical study of plastic overstrength of shear links. *Journal of Constructional Steel Research*, 82, 19–32. <https://doi.org/10.1016/j.jcsr.2012.11.013>
- Dusicka, P., & Lewis, G. (2010). High strength steel bolted connections with filler plates. *Journal of Constructional Steel Research*, 66(1), 75–84. <https://doi.org/10.1016/j.jcsr.2009.07.017>
- Egan, B., McCarthy, M. A., & McCarthy, C. T. (2017). Design, testing and analysis of bolted joints and connections. In *Comprehensive Composite Materials II* (pp. 178–205). Elsevier. <https://doi.org/10.1016/B978-0-12-803581-8.10056-6>
- Ghadami, A., Pourmoosavi, G., & Ghamari, A. (2021). Seismic design of elements outside of the short low-yield-point steel shear links. *Journal of Constructional Steel Research*, 178. <https://doi.org/10.1016/j.jcsr.2020.106489>
- Lian, M., Guan, B., Cheng, Q., Zhang, H., & Su, M. (2020). Experimental and numerical study of seismic performance of high-strength steel fabricated framed-tube structures with replaceable shear links. *Structures*, 28, 2714–2732. <https://doi.org/10.1016/j.istruc.2020.10.081>
- Mohammad Moradi, H., Hosseini Hashemi, B., & Jafari, M. A. (2020). Experimental and numerical study on the cyclic behavior of link-beam shear-panel connected to frame beams. *Engineering Structures*, 221. <https://doi.org/10.1016/j.engstruct.2020.111050>
- Mohebkah, A., & Azandariani, M. G. (2020). Shear resistance of retrofitted castellated link beams: Numerical and limit analysis approaches. *Engineering Structures*, 203. <https://doi.org/10.1016/j.engstruct.2019.109864>
- Musbar, M., Budiono, B., Kusumastuti, D., & Setio, H. D. (2018). Behavior of Modified Long Links with Supplemental Double Stiffeners on Eccentrically Braced Frames. *International Journal on Advanced Science, Engineering and Information Technology*, 8(6), 2516. <https://doi.org/10.18517/ijaseit.8.6.5852>
- Ramonell, C., & Chacón, R. (2021). On the topological optimization of horizontal links in eccentrically braced frames. *Journal of Constructional Steel Research*, 185. <https://doi.org/10.1016/j.jcsr.2021.106887>
- Richards, P. W., & Uang, C. M. (2005). Effect of Flange Width-Thickness Ratio on Eccentrically Braced Frames Link Cyclic Rotation Capacity. *Journal of Structural Engineering*, 131. <https://doi.org/10.1061/ASCE0733-94452005131:101546>
- Stephens, M., & Dusicka, P. (2014a). Analytical and numerical evaluation of continuously stiffened composite web shear links. *Journal of Structural Engineering (United States)*, 140(6). [https://doi.org/10.1061/\(ASCE\)ST.1943-541X.0001029](https://doi.org/10.1061/(ASCE)ST.1943-541X.0001029)

# Int. J of Mechanical, Materials and Industrial Engineering

Vol 2, No. 2, August 2023, ISSN 2964-8564

[www.orcaindustriakademi.com/ijmmie](http://www.orcaindustriakademi.com/ijmmie)

[doi.org/10.5281/zenodo.8199426](https://doi.org/10.5281/zenodo.8199426)

Stephens, M., & Dusicka, P. (2014b). Continuously stiffened composite web shear links: Tests and numerical model validation. *Journal of Structural Engineering (United States)*, *140*(7). [https://doi.org/10.1061/\(ASCE\)ST.1943-541X.0000996](https://doi.org/10.1061/(ASCE)ST.1943-541X.0000996)

Tian, X., Su, M., Lian, M., Wang, F., & Li, S. (2018). Seismic behavior of K-shaped eccentrically braced frames with high-strength steel: Shaking table testing and FEM analysis. *Journal of Constructional Steel Research*, *143*, 250–263. <https://doi.org/10.1016/j.jcsr.2017.12.030>

Zimbru, M., D’Aniello, M., Stratan, A., Landolfo, R., & Dubina, D. (2017). Finite element modelling of detachable short links. *COMPADYN 2017 - Proceedings of the 6th International Conference on Computational Methods in Structural Dynamics and Earthquake Engineering*, *1*, 790–801. <https://doi.org/10.7712/120117.5457.17470>